Prepared for submission to JCAP

arXiv:1403.6694v1 [astro-ph.CO] 26 Mar 2014

Standard big bang nucleosynthesis and primordial CNO Abundances after *Planck*

Alain Coc [a,1] **, Jean-Philippe Uzan**[b,c] **and Elisabeth Vangioni**[b,c]

[a]Centre de Sciences Nucléaires et de Sciences de la Matière (CSNSM), CNRS/IN2P3, Université Paris Sud 11, UMR 8609, Bâtiment 104, F–91405 Orsay Campus (France)

[b]Institut d'Astrophysique de Paris, UMR-7095 du CNRS, Université Pierre et Marie Curie, 98 bis bd Arago, 75014 Paris (France)

[c]Sorbonne Universités, Institut Lagrange de Paris, 98 bis bd Arago, 75014 Paris (France).

E-mail: coc@csnsm.in2p3.fr, uzan@iap.fr, vangioni@iap.fr

Abstract. Primordial or big bang nucleosynthesis (BBN) is one of the three historical strong evidences for the big bang model. The recent results by the *Planck* satellite mission have slightly changed the estimate of the baryonic density compared to the previous WMAP analysis. This article updates the BBN predictions for the light elements using the cosmological parameters determined by *Planck*, as well as an improvement of the nuclear network and new spectroscopic observations. The error bars of the primordial D/H abundance are narrower than previously and there is a slight lowering of the primordial Li/H abundance. However, this lithium value still remains typically 3 times larger than its observed spectroscopic abundance in halo stars of the Galaxy. In addition, for the first time, we provide confidence limits for the production of ^{6}Li, ^{9}Be, ^{11}B and CNO, resulting from our extensive Monte Carlo calculation with our extended network. A specific focus is cast on CNO primordial production. Considering uncertainties on the nuclear rates around the CNO formation, we obtain CNO/H $\approx (5-30)\times 10^{-15}$. We further improve this estimate by analysing correlations between yields and reaction rates and identifyed new infuential reaction rates. These uncertain rates, if *simultaneously* varied could lead to a significant increase of CNO production: CNO/H $\sim 10^{-13}$. This result is important for the study of population III star formation during the dark ages.

[1]Corresponding author.

Contents

1 Introduction **1**

2 Primitive observational abundances: update **2**
2.1 ^{4}He, D, ^{3}He and ^{7}Li observations 2
2.2 ^{6}Li, ^{9}Be, B, CNO observations 3

3 CMB parameters and consequences **4**

4 Method **5**
4.1 Monte Carlo 5
4.2 Reaction rates and uncertainties 7

5 Results concerning ^{4}He, D, ^{3}He and ^{7}Li **8**

6 Results concerning ^{6}Li, ^{9}Be, B, C **10**

7 Summary **15**

A Appendix: Relation between η and $\Omega_b h^2$ **16**

1 Introduction

There are three historical observational evidences for the big bang model: the cosmic expansion, the Cosmic Microwave Background (CMB) radiation and primordial or big bang nucleosynthesis (BBN). Today, they are complemented by a large number of evidences in particular from the properties of the large scale structures (see e.g. Ref. [43] for a textbook description). BBN predicts the primordial abundances of the "light cosmological nuclei": ^{4}He, D, ^{3}He and ^{7}Li that are produced during the first 20 min after the big bang when the Universe was dense and hot enough for nuclear reactions to take place. The comparison of the calculated and observed abundances shows an overall good agreement except for the ^{7}Li. The essential cosmological parameter of the model is the baryonic density Ω_b. It is related to the baryon to photon ratio, $\eta \equiv n_b/n_\gamma = 2.738 \times 10^{-8}\ \Omega_b h^2$ (see the appendix) that remains constant during the expansion after the electron–positron annihilation. $\Omega_b h^2$ is now well measured from the angular power spectrum of the CMB temperature anisotropies. A precise value for this, previously free, parameter was provided by the Wilkinson Microwave Anisotropy Probe (WMAP9) satellite, $\Omega_b h^2 = 0.02243 \pm 0.00055$, ("Nine-year (MASTER)", Hinshaw et al. [29]) while the recent *Planck* mission updated it to $\Omega_b h^2$=0.02218±0.00026 ("*Planck*+lensing+WP+highL", *Planck* Collaboration XVI [47]). We calculate here the ^{4}He, D, ^{3}He and ^{7}Li primordial abundances by Monte Carlo, using our extended 424 nuclear reaction network [15], also taking into account the updated value of the neutron lifetime [49]. In standard big bang nucleosynthesis, only traces of other isotopes are produced: ^{6}Li, ^{9}Be, ^{10}B, ^{11}B and CNO. The CNO abundance is of peculiar interest since it may affect Pop III stellar evolution in the first structures of the Universe. The value which could impact this evolution is estimated to be 10^{-11} [10] or even as low as 10^{-13} (in number of atoms relative to hydrogen, CNO/H) for the less massive stars [23]. In this context, it is important to evaluate

carefully the BBN CNO abundance. In our previous work [15] we obtained a much lower value CNO/H=0.7×10^{-15} but no upper nor lower limit (see also Ref. [33]). In this paper, we use the results of our Monte Carlo calculations *i*) to estimate the uncertainties on the BBN production of the minor isotopes, and in particular of CNO and *ii*) analyze the correlations between reaction rates and isotopic abundances to identify potentially important reactions that were not identified in our previous sensitivity analysis. We show that by calculating correlations, we find important reactions that were overlooked in sensitivity studies changing one reaction at a time. This is crucial because the level of the CNO abundance plays a key role in the evolution of the first stars.

2 Primitive observational abundances: update

2.1 ^{4}He, D, ^{3}He and ^{7}Li observations

Deuterium is a very fragile isotope, easily destroyed after BBN. Its most primitive abundance is determined from the observation of cosmological clouds at high redshift, on the line of sight of distant quasars. Very few such observations are available.

Up to now, the observation of about 10 quasar absorption systems gave the weighted mean abundance of deuterium D/H = $(3.02 \pm 0.23) \times 10^{-5}$ [41]. However, these individual measurements of D/H show a considerable scatter and it is likely that systematic errors dominate the uncertainties.

Recently, more precise observations of Damped Lyman-α (DLA) systems at high redshift have lead to provide [17, 45] a new mean value of

$$\mathrm{D/H} = (2.53 \pm 0.04) \times 10^{-5} \tag{2.1}$$

leading to a lower determination. We thus adopt this latter D/H mean abundance in our calculations. Due to this narrow error bar, adding other data with large error bars, do not change (only very slightly) this determination. However, we have to keep in mind possible systematic errors such which could alter this mean value [41].

After BBN, ^{4}He is still produced by stars, essentially during the main sequence phase. Its primitive abundance is deduced from observations in HII (ionized hydrogen) regions of compact blue galaxies. In a hierarchical structure formation model, these dwarf galaxies are more primitive than the present galaxies. The primordial ^{4}He mass fraction, Y_p, is obtained from the extrapolation to zero metallicity but is affected by systematic uncertainties [5, 34] such as plasma temperature or stellar absorption. Recently, Aver et al. [6, 7] have determined the primordial helium abundance using a Monte Carlo Markov Chain (MCMC) techniques. A regression to zero metallicity yields

$$Y_p = 0.2465 \pm 0.0097 \tag{2.2}$$

which corresponds to a narrower error bar than previous constraints. We take this latter value for comparison with our calculations. Note that another recent determination of Izotov et al. [35] is $Y_p = 0.254 \pm 0.003$, which is somewhat higher than the Aver et al value.

Contrary to ^{4}He , ^{3}He is both produced and destroyed in stars all along its galactic evolution, so that the evolution of its abundance as a function of time is subject to large uncertainties. Moreover, ^{3}He has been observed in our Galaxy [8], and one only gets a 'local' constraint

$$^3\mathrm{He/H} = (1.1 \pm 0.2) \times 10^{-5}. \tag{2.3}$$

Consequently, the baryometric status of ^{3}He is not firmly established [64].

Primitive lithium abundance is deduced from observations of low metallicity stars in the halo of our Galaxy where the lithium abundance is almost independent of metallicity, displaying the so-called Spite plateau [57]. This interpretation assumes that lithium has not been depleted at the surface of these stars, so that the presently observed abundance can be assumed to be equal to the primitive one. The small scatter of values around the Spite plateau is indeed an indication that depletion may not have been very efficient. However, there is a discrepancy between the value *i)* deduced from these observed spectroscopic abundances and *ii)* the BBN theoretical predictions assuming $\Omega_{\rm b}$ is determined by the CMB observations. Many studies have been devoted to the resolution of this so-called *Lithium problem* and many possible "solutions", none fully satisfactory, have been proposed. For a detailed analysis see Fields [24], the proceedings of the meeting "Lithium in the cosmos" [32] and recently Cyburt et al. [19]. Note that recent lithium observations [30] have been done in the Small Magellanic Cloud which is a nearby irregular galaxy with quarter of the sun's metallicity and its abundance is found to be nearly equal to the BBN one. It could be a strong constraint for the lithium galactic evolution.

Astronomical observations of these metal poor halo stars [51] have thus led to a relative primordial abundance of Li/H = $(1.23^{+0.34}_{-0.16}) \times 10^{-10}$ while a more recent analysis [53] gives

$$\mathrm{Li/H} = (1.58 \pm 0.31) \times 10^{-10} \tag{2.4}$$

which we use in our analysis. For reviews on the Li observations, we refer to Spite & Spite [58] and Frebel & Norris [25].

2.2 ^{6}Li, ^{9}Be, B, CNO observations

The origin of the light elements LiBeB, is a crossing point between optical and gamma spectroscopy, non thermal nucleosynthesis (via spallation with Galactic Cosmic Rays, GCR), stellar evolution and Big Bang nucleosynthesis. As said above for ^{7}Li , ^{6}Li is also observed in metal poor stars. Its observational story is peculiar. In the past, Asplund et al. [3] have provided observations of ^{6}Li /^{7}Li ratio which suggesting the presence of a plateau, typically ^{6}Li/H = 10^{-11} leading to a possible pre-galactic origin of this isotope (see Rollinde et al. [50]). In this context, a new measurement of the D(α,γ) ^{6}Li which is the main way to produce primordial ^{6}Li has been performed (Hammache et al. [28]). This study has confirmed the low primordial value, ^{6}Li/H = 10^{-14}. In a second time, the observational ^{6}Li plateau has been questioned in Cayrel et al. [11] due to line asymmetries which were neglected in previous abundance analysis. Presently, only one star, HD84937, presents a ^{6}Li/^{7}Li ratio of the order of 0.05 (see Lind et al. [37], Steffen et al. [59]) and there is no remaining evidence for a plateau at very low metallicity. We hence use this value as an upper limit: ^{6}Li/H$\lesssim 10^{-11}$.

Beryllium has only one isotope. As D and Li, it is a fragile nucleus. It is formed in the vicinity of Type II supernovae (SNII) by non thermal process (spallation) (see Vangioni-Flam et al. [61, 62]). It is also observed in metal poor stars. Boesgaard et al. [9] (and references therein) have performed an update of Be observations in metal poor stars which provides a primitive abundance at very low metallicity of the order of Be/H = $3. \times 10^{-14}$ at [Fe/H] = -3.5. This observation, that we adopt as upper limit of the primordial abundance, has to be compared to the typical primordial Be abundance, Be/H = 10^{-18}.

Boron has two isotopes: ^{10}B and ^{11}B. It is also synthesized by non thermal processes, GCR or neutrinos (for ^{11}B) (see Vangioni-Flam et al. [60, 61], Vangioni-Flam & Cassé [63]).

The most recent observations of boron in low metal stars come from Duncan et al. [22] and Garcia-Lopez et al. [26]. In the galactic halo, the lowest boron abundance at [Fe/H] $\lesssim$ -3. is B/H$\approx 10^{-12}$, to be compared to the typical primordial B abundance B/H $= 3. \times 10^{-16}$.

For a general review of these light elements, see the IAU Proceedings Edts Charbonnel et al. [12].

Finally, CNO elements are observed in the lowest metal poor stars (around [Fe/H]=-5). The observed abundance of CNO is typically [CNO/H]= -4, relatively to the solar abundance i.e. primitive CNO/H$< 10^{-7}$. For a review see Frebel & Norris [25] and references therein.

3 CMB parameters and consequences

Concerning the update of the CMB, a comparison between the columns of Table 1 shows the effect of a change in $\Omega_{\rm b}h^2$ from Spergel et al. [55] to Komatsu et al. [36] (columns 2 and 3) and from Komatsu et al. [36] to *Planck* Collaboration XVI [47] (columns 4 and 5). It mostly affects ^{7}Li/H by about 4% and D/H by about 2.7% while the other changes are below a percent.

A BBN evaluation has been done by *Planck* Collaboration XVI [47], using $\Omega_{\rm b}h^2=$ 0.02207±0.00027; their prediction regarding the Y_p and D/H abundances are similar to ours (0.24725±0.00032 and 2.656±0.067 $\times 10^{-5}$ respectively at $\eta_{\rm CMB}$) but they do not provide any ^{7}Li/H value.

Table 1. Primordial abundances with reduced network. (Bold face displayed values highlight parameter changes.)

	(a)	(b)	This work	This work
Nb. reactions	13	15	15	15
$\Omega_{\rm b}h^2$	$0.0223^{+0.00075}_{-0.00073}$ (c)	**0.02249** (e)	0.02249 (e)	**0.02207 (g)**
$\tau_{\rm n}$	885.7±0.8 (d)	885.7 (d)	**880.1 (f)**	880.1
Y_p	0.2476±0.0004	0.2475	0.2464	0.2462
D/H ($\times 10^{-5}$)	2.68 ± 0.15	2.64	2.64	2.72
^{3}He/H ($\times 10^{-5}$)	1.05±0.04	1.05	1.05	1.06
^{7}Li/H ($\times 10^{-10}$)	5.14±0.50	5.20	5.18	4.98

(a) Coc & Vangioni [13]; (b) Coc et al. [15], (c) Spergel et al. [55] ; (d) Amsler et al. [48]; (e) Komatsu et al. [36] ; (f) Beringer et al. [49]; (g) *Planck* Collaboration XVI [47]

A recent paper by Pizzone et al. [46] provides new evaluation of ^{4}He, D, ^{3}He and ^{7}Li primordial abundances based on new nuclear data, but comparison with this work is difficult. The new data is extracted by an *indirect* experimental method (the Trojan Horse Method) that requires theoretical input. We use instead the results of *direct measurements that provide the same data at, and even below, BBN energies* [20], not affected by screening [65]. Their neutron lifetime value is a peculiar choice (the Serebrov et al. [54] experimental result only) but their η value is now outdated (WMAP seven years [36]). More important for a relevant comparison, is that nothing is said of the origin for rate of the ^{3}He$(\alpha,\gamma)^7$Be used in their calculations, which is known to be essential for ^{7}Li prediction, and has been updated by Cyburt & Davids [18].

Table 2. Primordial abundances with extended network.

Nb. reactions	424	424	424
$\Omega_{\rm b}h^2$	0.02243 (x)	0.02207 (y)	0.02218±0.00026 (z)
$\tau_{\rm n}$	880.1	880.1	880.1±1.1
Y_p	0.2465	0.2463	0.2461–0.2466
D/H ($\times 10^{-5}$)	2.60	2.67	2.57–2.72
^{3}He/H ($\times 10^{-5}$)	1.04	1.05	1.02–1.08
^{7}Li/H ($\times 10^{-10}$)	5.13	4.96	4.56–5.34

(x) Inshaw et al., WMAP9 [29] (y) *Planck* only [47] (z) *Planck*+lensing+WP+highL [47]

Table 3. Comparison with observations

	This work	Observations
Y_p	0.2461–0.2466	0.2465 ± 0.0097
D/H ($\times 10^{-5}$)	2.57–2.72	2.53 ± 0.04
^{3}He/H ($\times 10^{-5}$)	1.02–1.08	1.1 ± 0.2
^{7}Li/H ($\times 10^{-10}$)	4.56–5.34	1.58 ± 0.31

4 Method

4.1 Monte Carlo

Coc & Vangioni [13] used a network reduced to the 12 main reactions (13 with the ^{3}H(p,γ)^{4}He that plays a negligible role) for which the rate uncertainties are small compared to all other ones, and sampled the rates within the uncertainty range according to a normal distribution. Here, the extended network includes reaction rates that can be uncertain by a factor of a few orders of magnitude due to the lack of experimental data. Hence, we follow Longland et al. [38] and use a lognormal distribution to cope with these large uncertainty factors together with ensuring that the sampled rates are positive:

$$f(x) = \frac{1}{\sigma\sqrt{2\pi}}\frac{1}{x}e^{-(\ln x-\mu)^2/(2\sigma^2)} \tag{4.1}$$

(with $x \equiv N_A\langle\sigma v\rangle$ for short). This is equivalent to assumption that $\ln(x)$ is Gaussian distributed with expectation value μ and variance σ^2. For the lognormal distribution, one has:

$$E[x] = e^{(2\mu+\sigma^2)/2}, \quad \text{and} \quad V[x] = e^{(2\mu+\sigma^2)}\left[e^{\sigma^2}-1\right]. \tag{4.2}$$

As discussed in Longland et al. [38] (see their Fig. 1), for small σ a lognormal distribution and a normal distribution with the same expectation value and variance are close to each other. Hence, since the uncertainty in the 12 main reaction rates are small, using here a lognormal distribution for those reactions makes no difference with Coc & Vangioni [13] results.

To perform the Monte Carlo calculation, we follow the prescription of Sallaska et al. [52]. Namely the reaction rates $x_k \equiv N_A\langle\sigma v\rangle_k$, (with k being the index of the reaction), are

assumed to follow a lognormal distribution:

$$x_k(T) = \exp\left(\mu_k(T) + p_k \sigma_k(T)\right) \tag{4.3}$$

where p_k is sampled according to a *normal* distribution of mean 0 and variance 1 (Eq. (22) of Sallaska et al. [52]). μ_k and σ_k determine the location of the distribution and its width which are tabulated as a function of T:

$$x_{\rm med} \equiv \exp\left(\mu\right) \tag{4.4}$$

is the median rate and

$$f \equiv \exp\left(\sigma\right) \tag{4.5}$$

the uncertainty factor. They are deduced from the evaluation of rate uncertainties. For reactions for which high and low rates are available,

$$\mu \equiv \ln \sqrt{x_{\rm low} \times x_{\rm high}} \tag{4.6}$$

and

$$\sigma \equiv \ln \sqrt{x_{\rm high}/x_{\rm low}} \tag{4.7}$$

(see Longland et al. [38]). To avoid erratic numerical behavior, we limit the sampling to values lower than one thousand times the median rate, i.e.,

$$x < 10^3\ x_{\rm med}, \tag{4.8}$$

to remain within a range already explored [15].

The Monte Carlo calculation proceeds as follows. For each trial labeled by i, we sample randomly a set of $\{p_{k;i}\}$ different numbers where k that runs from 1 to N (number of reactions) is the index of the reaction. Each one follows independently a Gaussian distribution of mean value 0 and variance 1 and is obtained from a standard random number generator. A BBN calculation is performed with the set of reaction rates $\{x_{k;i}\}$ obtained from Eq. (4.3) that produce the set of isotopic abundances $\{y_{j;i}\}$ obtained in trial i. Here, j=^{4}He, D, ^{3}He, ^{7}Li, ^{6}Li, ^{9}Be, ^{11}B and CNO is the index the corresponding abundances after decays of radioactive isotopes (^{7}Be, ^{3}H, ^{11}C, ...) or summation of A$\geq$12 isotopic abundances (CNO).

To obtain the primordial abundances and their uncertainties, as tabulated below, $\Omega_{\rm b}h^2$ also is randomly sampled, following a Gaussian distribution according to the CMB deduced data. After 30000 such computations, the calculated distributions of abundances are obtained as displayed in Fig. 1 for ^{7}Li. The median primordial abundances and associated 68% confidence intervals are then calculated by taking respectively the 0.5, 0.16 and 0.84 quantiles of the abundance distributions (see Fig. 5 in Longland et al. [38]).

It has recently been recognized that traditional sensitivity studies, in which only one reaction is varied while the others are held constant, cannot properly address all the important correlations between rate uncertainties and nucleosynthetic predictions. Sensitivity studies can be improved by searching for such correlations as was done by Parikh et al. [42] for X–ray bursts (see their Figs. 7 and 8). For this purpose, the same Monte Carlo calculation is performed, except that $\Omega_{\rm b}h^2$ is fixed, to obtain a data base that can be used to study correlations. The correlation coefficient between isotope j and reaction k is, then, calculated as:

$$C_{j,k} = \frac{1}{N} \frac{\sum_{i=1}^{N} \left(y_{j;i}\ p_{k;i} - \overline{y_j}\ \overline{p_k}\right)}{\sigma_j \sigma'_k} \tag{4.9}$$

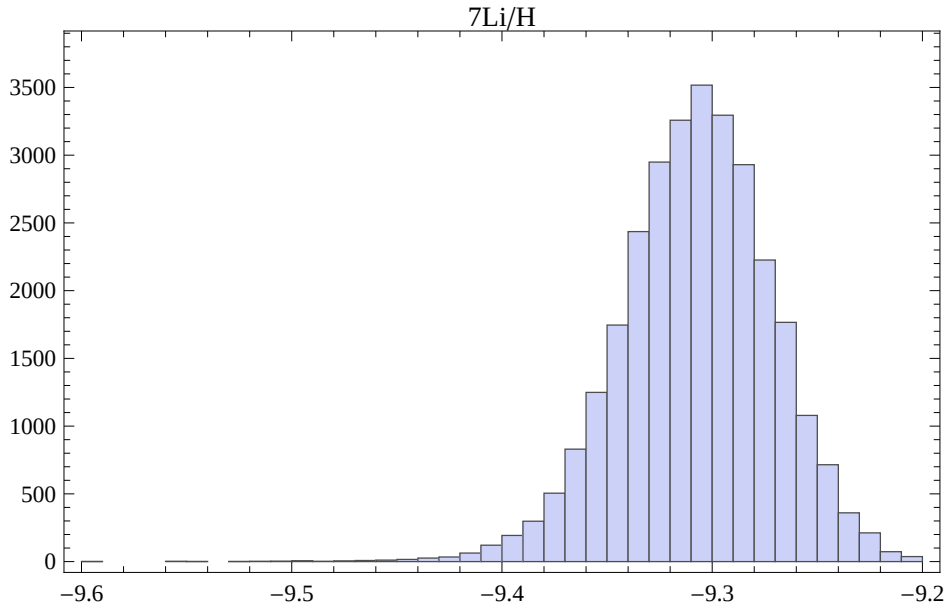

Figure 1. Histogram of the ^{7}Li/H distribution, from which the median and confidence interval is calculated.

where $y_{j;i}$ is again the final abundance of isotope j obtained in trial i with the set of reaction rates $\{x_{k;i}\}$ obtained from Eq. (4.3) with the set of randomly sampled $\{p_{k;i}\}$. The correlation coefficients are calculated, with $y_j \equiv \ln(n_j/n_H)$ for $j \neq^4$He and $y_{^4\mathrm{He}} \equiv Y_p$ for the abundances. In Eq. (4.9), $\overline{y_j}$ [$\overline{p_k}$] and σ_j [σ'_k] stand for the mean and standard deviation of y_j [p_k]. If it were not for the condition (4.8), one would have obviously $\overline{p_k} \equiv 0$ and $\sigma'_k \equiv 1$ since the p_k are sampled according to a normal distribution.

4.2 Reaction rates and uncertainties

In this study, the reaction network and the thermonuclear rates comes from Coc et al. [15]. Namely, it includes 59 nuclides from neutron to ^{23}Na, linked by 391 reactions involving n, p, d, t and ^{3}He induced reactions and 33 β-decay processes [4]. Reaction rates were taken primarily from Angulo et al. [2], Descouvemont et al. [20], Iliadis et al. [31], Xu et al. [67] and other evaluations when available. Following their sensitivity study a few reaction rates were re-evaluated by Coc et al. [15]; they are also used here. The complete list of reactions with associated references to the origin of the rates can be found in Table 4 of Coc et al. [15]. Since our previous Monte Carlo BBN calculations [13], no change has been made concerning 11 of the 12 main BBN reactions rates. We thus use those from the evaluation performed by Descouvemont et al. [20] except for ^{1}H(n,γ)D [1] and ^{3}He$(\alpha,\gamma)^7$Be [18]. The only modification of the main rates concerns the weak reactions involved in n$\leftrightarrow$p equilibrium whose rates [21] is determined from the standard theory of the weak interaction but needs to be normalized to the experimental neutron lifetime. The latter has recently been revised by the Particle Data Group from 885.7$\pm$0.8 s [48], used in Coc & Vangioni [13], to 880.1$\pm$1.1 s [49]. This significant change is due to the re-consideration of a previously discarded [54] experimental value, now comforted by new analyses (see Beringer et al. [49], Wietfeldt & Greene [66] for more details). For this quantity, we use the latest value recommended by the

Particle Data Group $\tau_n = 880.1 \pm 1.1$ s [49], but are aware that this remains an open debate [Yue et al. [68] recently propose τ_n=887.7±1.2(stat)±1.9(syst)] that affects essentially, only ^{4}He.

For the remaining of the 391 reactions, we use tabulated μ and σ [31], tabulated limits [2, 15, 20, 67] together with Eqs. (4.6) and (4.7) and for the others, tabulated rates together with estimated uncertainty factors and Eqs. (4.4) and (4.5). In particular, in the work of Coc et al. [15], many rates come from theory [27] and have not been re-evaluated since then, in this sensitivity study, they were not found to influence significantly the results, when *individually* multiplied by factors up to $10^{\pm 3}$. These factors come from the comparison [15] between TALYS calculations and experimentally determined reaction rates. For those rates, labeled "TALYS" in Table 4 of Coc et al. [15], we use here uncertainty factors of f=100 (i.e. $\sigma = \ln(100)$). (Those, labeled "TALYS" in bold face in the same Table were re-evaluated so that calculated uncertainties are available.) For rates provided without calculated uncertainty, labeled e.g. "CF88", "MF89", "Wag69",..., (see Refs. in Coc et al. [15]) we generally adopted f=3, except when the uncertainty is not provided but is obviously smaller e.g. "Ham10" [28] or "Nag06" where we adopted a 40% uncertainty (f=1.4). This may look arbitrary, but one of the main goal of this work is to identify potentially influential reaction rates that may have to be improved in a subsequent stage.

5 Results concerning ^{4}He, D, ^{3}He and ^{7}Li

Figure 2 displays the ^{4}He, D, ^{3}He and ^{7}Li abundances calculated as a function of η by Monte Carlo with the full network, and evaluated rate uncertainties following Coc et al. [15], compared to our previous work with a reduced network [13]. At $\eta_{\rm CMB}$, the differences are hardly visible except for ^{4}He, due to the updated neutron lifetime.

Hence, comparison between columns 2 and 5 in Table 1 shows the evolution of the yields from Coc & Vangioni [13] with the first WMAP results [55] to the recent *Planck* data [47]. The reduced uncertainty on D/H is a direct consequence of the reduced uncertainty on $\Omega_b h^2$ while ^{7}Li uncertainty is still dominated by nuclear uncertainty on the ^{3}He$(\alpha,\gamma)^7$Be rate.

Since the neutron lifetime and baryonic density values are both subject to debate (Beringer et al. [49] and Yue et al. [68] for τ_n and *Planck* Collaboration XVI [47] and Spergel et al. [56] for $\Omega_b h^2$), instead of providing new tabulated values, we propose fits for the BBN abundances of ^{4}He, D, ^{3}He and ^{7}Li abundances as a function of $\Omega_b h^2$, τ_n and $N_{\rm eff}$ (see definition below) hence of the BBN predictions. This can be used to update any column of Tables 1 and 2 with $\Omega_b h^2$ or τ_n different values than those in the same column or for $\Delta N_{\rm eff} = N_{\rm eff} - 3 \neq 0$.

$$\begin{aligned} \Delta Y_p = {} & +0.4274\ \Delta\Omega_b h^2 + 2.043 \times 10^{-4}\ \Delta\tau_n + \\ & 1.348 \times 10^{-2}\ \Delta N_{\rm eff} - 9.805 \times 10^{-4}\ \Delta N_{\rm eff}^2 \end{aligned} \tag{5.1}$$

$$\Delta {\rm D/H} = -1.878 \times 10^{-3}\ \Delta\Omega_b h^2 + 1.256 \times 10^{-8}\ \Delta\tau_n + 3.564 \times 10^{-6}\ \Delta N_{\rm eff}, \tag{5.2}$$

$$\Delta\, ^3{\rm He/H} = -2.783 \times 10^{-4}\ \Delta\Omega_b h^2 + 1.761 \times 10^{-9}\ \Delta\tau_n + 5.064 \times 10^{-7}\ \Delta N_{\rm eff}, \tag{5.3}$$

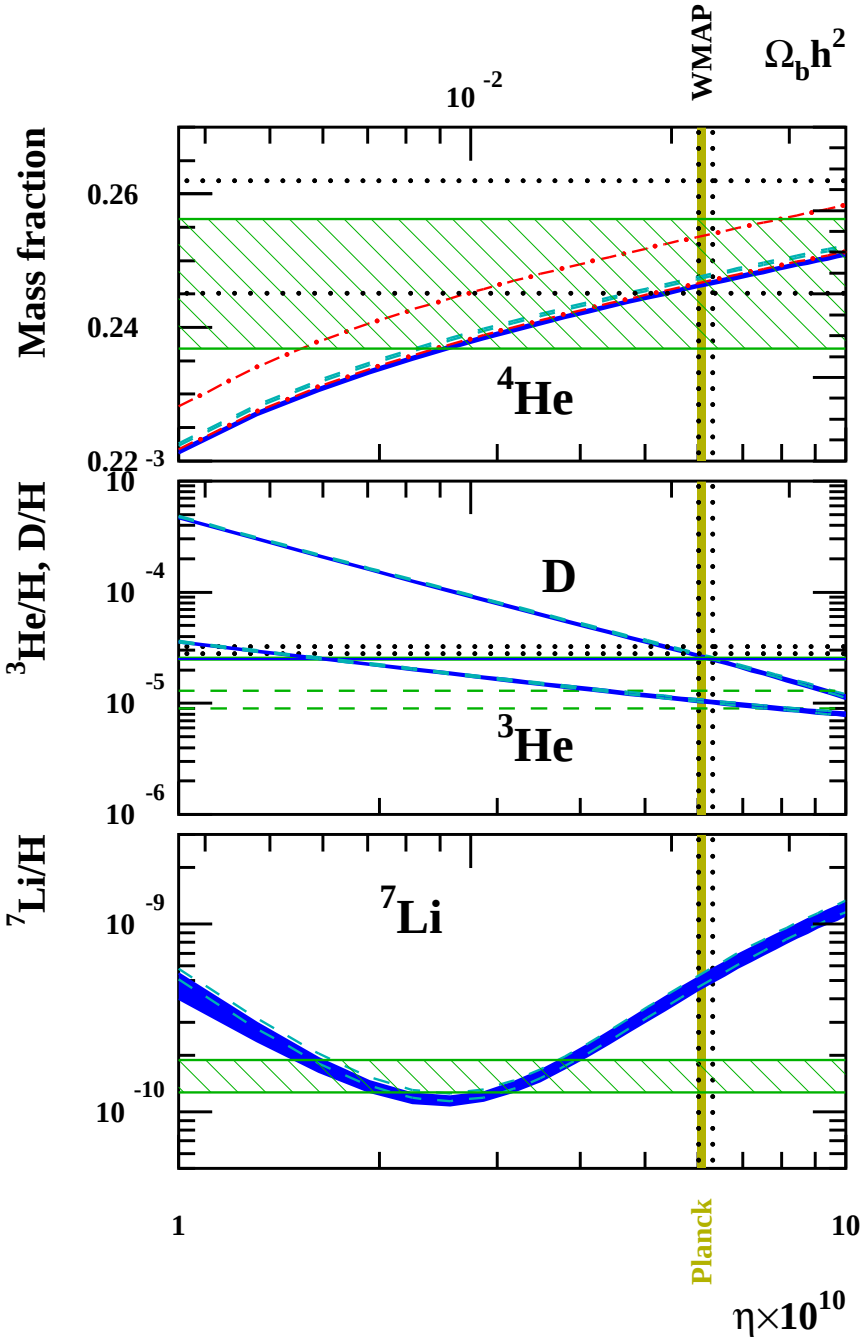

Figure 2. (Color online) ^{4}He, D, ^{3}He and ^{7}Li abundances as a function of η calculated by Monte Carlo with the updated full network (dark blue) or with the reduced network as in Ref. [13] (light blue dashed). The vertical areas correspond i) to the WMAP (dot, black) and ii) *Planck* (solid, yellow) baryonic densities. The horizontal areas (hatched green) represent the adopted observational abundances while the horizontal dotted lines correspond to those previously used [6, 41]. The (red) dash–dotted lines correspond to Y_p calculated with $N_{\rm eff} = 3.30 \pm 0.27$ derived from the CMB [47].

$$\Delta^7\mathrm{Li/H} = +4.767 \times 10^{-8}\ \Delta\Omega_\mathrm{b}h^2 + 2.4541 \times 10^{-13}\ \Delta\tau_\mathrm{n} - 4.686 \times 10^{-11}\ \Delta N_\mathrm{eff}. \quad (5.4)$$

These fits also consider the variations induced by a change in $-1 < \Delta N_\mathrm{eff} < +1$ where N_eff, the effective number of relativistic degrees of freedom, is defined by:

$$\rho_\mathrm{r} = \left[1 + \frac{7}{8} N_\mathrm{eff} \left(\frac{T_\nu}{T}\right)^4 + \frac{15}{\pi^2}\frac{\rho_e}{T^4}\right] \rho_\gamma. \quad (5.5)$$

At recombination, $\rho_e \ll \rho_\mathrm{r}$ and $(T_\nu/T)^4 = (4/11)^{4/3}$, so that Eq. (5.5) matches the definition used in CMB analyses.

Figure 2 displays the abundances as a function of η and Table 3 those at the *Planck* baryonic density, both for $N_\mathrm{eff} = 3$. We do not use the $N_\mathrm{eff} = 3.046$ value from Mangano et al. [40] to account for non–instantaneous neutrino decoupling in the presence of oscillations. While this approximation works for ^{4}He, the change for the other nuclides is exactly in the opposite direction of the true one. Hence, to implement these very small effects ($\approx 2 \times 10^{-4}$ for Y_p), we suggest the interested reader to correct $N_\mathrm{eff} = 3$ results (i.e. Table 3) with the exactly calculated abundance changes (e.g. ΔY_p) given in the Tables of Mangano et al. [40], rather than considering $N_\mathrm{eff} = 3.046$ results. The high precision calculation of ^{4}He primordial abundances also requires corrections to the weak rates [39]. We have introduced the dominant contribution (Coulomb and zero temperature radiative corrections) that induce a +1.28% shift of Y_p [39] but at present, not the others (+0.72%) because of the larger uncertainties in the ^{4}He observations. With these limitations, and using the last evaluation of Y_p [7], we obtain $2.67 \leq N_\mathrm{eff} \leq 3.77$ at *Planck* baryonic density, with N_eff defined by Eq. (5.5). [Note that in Coc et al. [16] we obtained $2.89 \leq N_\mathrm{eff} \leq 4.22$ corresponding to the previous evaluation of Y_p [6].] In Figure 2 we also display for visual inspection the results obtained for the limits on effective number of neutrino family $N_\mathrm{eff} = 3.30 \pm 0.27$ derived from the CMB only confidence interval [47]. Finally in Table 3, a comparison between this work and the last observational data is proposed; an overall consistency between standard BBN calculation and the observational constraints is presented except for lithium, as explained above: the discrepancy remains of the order of 3.

6 Results concerning ^{6}Li, ^{9}Be, B, C

Figure 3 displays the ^{6}Li, ^{9}Be, ^{10}B, ^{11}B and CNO abundances calculated as a function of η including our estimated uncertainties from the Monte Carlo, and a comparison with observations. The displayed uncertainties are obtained by calculating for each value of η, the 0.16 and 0.84 quantile [38] of the distributions. The corresponding confidence intervals at η_CMB are displayed in Table 4 and are orders of magnitude below observations (§ 2.2).

Figure 4 displays the histogram of CNO/H obtained from our Monte Carlo calculation, from which it is possible to extract the 0.16, 0.5 and 0.84 quantile, respectively given by 4.94×10^{-16}, 9.63×10^{-16} and 2.85×10^{-15}. This is very close to the range CNO/H = $(0.5 - 3.) \times 10^{-15}$ estimated by Coc et al. [14] from the results of Coc et al. [15]. However, at high value, the tail of the distribution extends to values much above the CNO/H = 10^{-13} limit. One can easily isolate and extract this subset from the database, but since all ≈400 reaction rates are different from one trial to the other, it was not possible to identify the combination reaction rates that produced such an effect. To identify those combinations of reaction rates

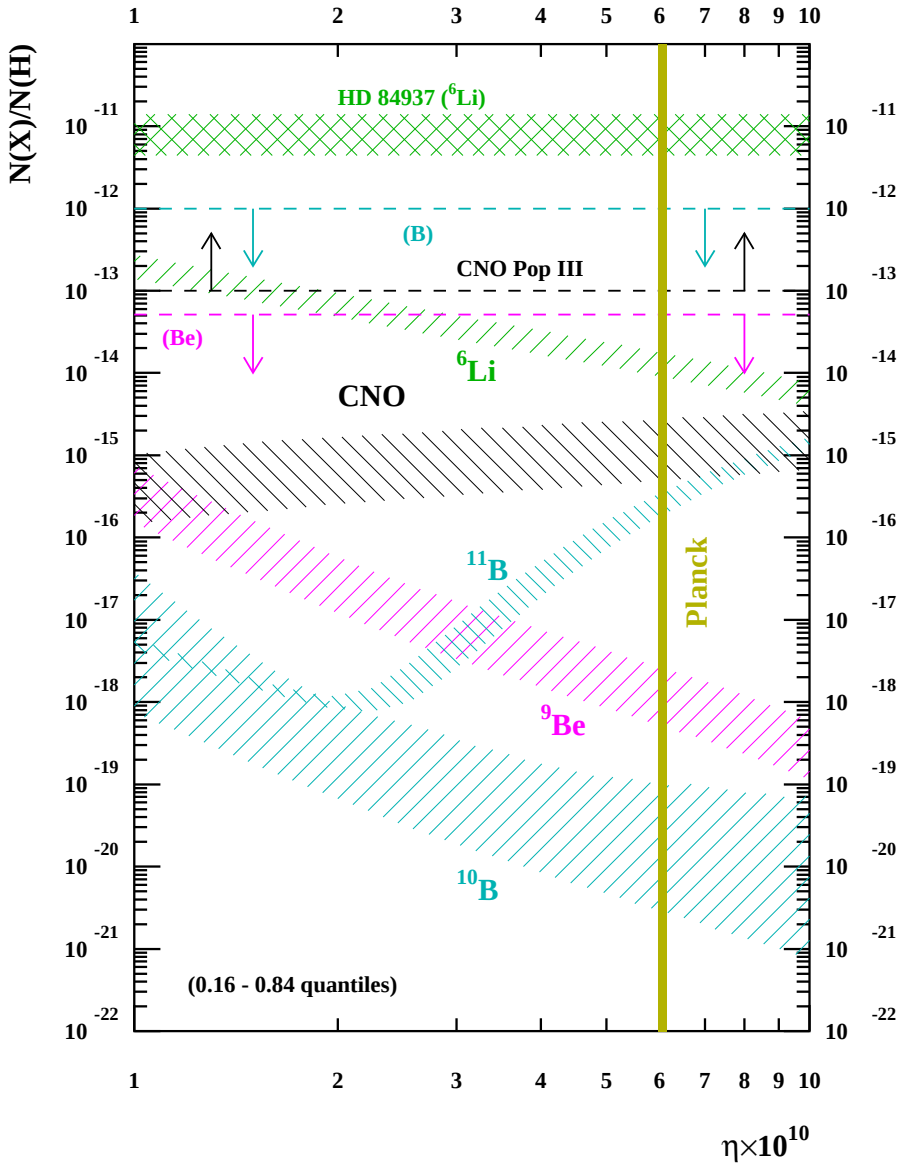

Figure 3. Standard big bang Nucleosynthesis predictions for the abundances of ^{6}Li, Be, B and CNO isotopes as a function of baryonic density, compared to some observations. The horizontal lines and areas correspond to the ^{6}Li observation in HD 84937 (green), beryllium (magenta) and boron (light blue) upper limits, and CNO lower limit to affect Population III stars; see text.

that allows such high value, we relied upon the calculated correlations between rates and yields.

This method is complementary to the one used by Coc et al. [15], in which a single reaction was tested at a time by changing its rate by factors of 10^n, $n = -3, -2, -1, 1, 2, 3$. Here all rates are simultaneously changed by factors, different for each reaction, and randomly sampled as described above. This allows to identify sub-networks rather than individual

Table 4. ^{6}Li to CNO primordial abundances by number.

	Ref. [15]	This work
^{6}Li/H ($\times 10^{-14}$)	1.23	0.90–1.77
^{9}Be/H ($\times 10^{-19}$)	9.60	5.10–26.3
^{11}B/H ($\times 10^{-16}$)	3.05	1.85–3.56
CNO/H ($\times 10^{-16}$)	7.43	4.94–28.5

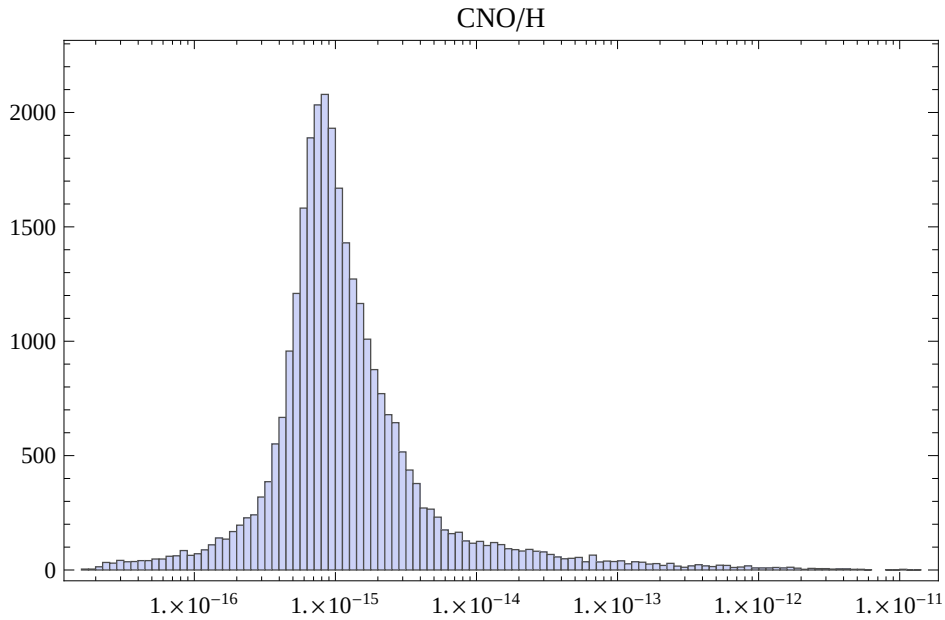

Figure 4. CNO/H distribution showing that high values are obtained in a non negligible proportion.

reactions and takes into account the different uncertainty factors. Results are displayed in Tables 5–12 when their absolute value exceed 10%. Note however that a higher sensitivity, as calculated in Coc & Vangioni [13], Coc et al. [15], does not necessarily correspond to a higher correlation as calculated here. Our previous sensitivity studies assumed an arbitrary ±15% rate variation [13] or a factor of up to 1000 rate variation [15]. Here, while, when sampling the rates, we still allow for large arbitrary rate variations for reactions with no documented rate uncertainties, we restrict the variations to evaluated rates and associated uncertainties when available. These latter reactions include e.g. those evaluated by Descouvemont et al. [20] or those identified as influential in a first step, but evaluated in a second step by Coc et al. [15]. For instance, the most influential rate on ^{7}Li+^{7}Be is ^{1}H(n,γ)^{2}H [13] but its rate uncertainty is very small [1] so that it does not appear in the table, contrary to the next most influential, ^{3}He(α,γ)^{7}Be whose rate uncertainty is still not negligible and thus appears in Table 8.

The reactions that appear most correlated with the isotopes lighter than C (Tables 5–11) are among those found in previous studies. In Table 12, it appears that besides the already known influential reactions on CNO production [15] [^{7}Li(d,n)2^{4}He, ^{12}B(p,α)^{9}Be,

^{8}Li(α,n)^{11}B, ^{13}C(d,α)^{11}B], new influential reactions are found. It indicates a new possible path for CNO production involving ^{10}Be, namely: ^{10}Be(p,α)^{7}Li, ^{10}Be(α,n)^{13}C, ^{7}Li(t,γ)^{10}Be, ^{8}Li(t,n)^{10}Be, ^{10}Be(t,n)^{12}B and ^{10}Be(p,t)2^{4}He. Note that all these new reactions involve radioactive isotope(s) [^{3}H, ^{8}Li and ^{10}Be] in the initial state, hence the absence of direct experimental data. From this analysis, it is obvious that a new chain of reactions leading to CNO via ^{10}Be need further attention as it could, depending on the cross-sections, provide a more efficient source of CNO.

Table 5. Correlations with ^{4}He

Reaction	$C_{\mathrm{He4},k}$
$1/\tau_{\mathrm{n}}$	-0.9677
^{3}He(t,np)^{4}He	0.1151
D(d,n)^{3}He	0.1282
D(d,p)^{3}H	0.1296

Table 6. Correlations with D

Reaction	$C_{\mathrm{D},k}$
D(p,γ)^{3}He	-0.7790
D(d,n)^{3}He	-0.4656
D(d,p)^{3}H	-0.4082

Table 7. Correlations with ^{3}He

Reaction	$C_{\mathrm{He3},k}$
D(p,γ)^{3}He	0.6699
D(d,n)^{3}He	0.1640
D(d,p)^{3}H	-0.1897
^{3}He(d,p)^{4}He	-0.6841

Table 8. Correlations with ^{7}Li

Reaction	$C_{\mathrm{Li7},k}$
^{7}Be(n,α)^{4}He	-0.3057
^{7}Be(d,p)2^{4}He	-0.2079
D(p,γ)^{3}He	0.4043
D(d,n)^{3}He	0.1547
^{3}He(d,p)^{4}He	-0.2232
^{3}He(α,γ)^{7}Be	0.7107

Table 9. Correlations with ^{6}Li

Reaction	$C_{\mathrm{Li6},k}$
D(α,γ)^{6}Li	0.9835
^{6}Li(p,α)^{3}He	-0.1333

Table 10. Correlations with ^{9}Be

Reaction	$C_{\mathrm{Be9},k}$
^{7}Li(^{3}He,p)^{9}Be	0.2820
^{7}Li(t,n)^{9}Be	0.8910

Table 11. Correlations with ^{11}B

Reaction	$C_{\mathrm{B11},k}$
^{11}B+^{11}C	
D(p,γ)^{3}He	0.1081
^{3}He(α,γ)^{7}Be	0.1621
^{7}Be(α,γ)^{11}C	0.2188
^{11}C(n,α)2^{4}He	-0.9069

Table 12. Correlations with CNO

Reaction	$C_{\mathrm{CNO},k}$
CNO	
^{12}B(p,α)^{9}Be	-0.1030
^{10}Be(p,α)^{7}Li	-0.2479
^{10}Be(α,n)^{13}C	0.2175
^{7}Li(t,γ)^{10}Be	0.1363
^{8}Li(α,n)^{11}B	0.1449
^{8}Li(t,n)^{10}Be	0.1958
^{10}Be(t,n)^{12}B	0.1139
^{13}C(d,α)^{11}B	-0.2378
^{10}Be(p,t)2^{4}He	-0.1297
^{7}Li(d,n)2^{4}He	-0.1806

These reactions were not identified in our previous work [15], because we varied the rates, *one at a time*, (by factors of 10^n with n varying from -3 to 3 by steps of one unit). Here, we first allowed *all rates to vary simultaneously and independently* according to lognormal distributions. Now, to better identify the chains of reactions that may lead to an increased CNO production, we allow the rates of the 6 newly identified reactions listed above to vary within a few orders of magnitude as in Ref. [15] but considering *all* possible combinations. We chose factors of $10^{\pm 2}$ variations on rates w.r.t. TALYS calculated rates which are consistent with our comparison between TALYS and experimentally measured rates [15] and select those combinations of factors that leads to a CNO/H production higher than 10^{-13}, the minimum value to affect Pop III stars [23]. In Table 13 are displayed the 9 combinations (out of $3^6 = 729$ combinations) of signs in the exponent of the$10^{\pm 2}$ factors (with "0" meaning no rate variation) for which CNO/H $> 10^{-13}$. Table 13, shows that the ^{7}Li(t,γ)^{10}Be and ^{10}Be(t,n)^{12}B reactions are not essential since whatever the exponent (-2, 0 or +2) of the variation factor, the result is not significantly affected. On the contrary, the combination of higher rates for ^{10}Be(α,n)^{13}C and ^{8}Li(t,n)^{10}Be together with lower rates for ^{10}Be(p,α)^{7}Li and ^{10}Be(p,t)2^{4}He result in a substantial increase in primordial CNO production. The factors of $10^{\pm 2}$ variation w.r.t. TALYS rates is conservative (see again Figs. 1–11 and 16–21 in Ref. [15]) so that even higher CNO yields can be expected. Experimental investigations of these four reactions (Fig. 5) are hence highly recommended.

Table 13. Each column correspond to a combination of multiplicative factors ("-" for 10^{-2}, "0" for 10^{0} and "+" for 10^{+2}) which applied simultaneously to all the six TALYS reaction rates lead to CNO/H$> 10^{-13}$.

Reaction	CNO/H$> 10^{-13}$								
^{10}Be(p,α)^{7}Li	-	-	-	-	-	-	-	-	-
^{10}Be(α,n)^{13}C	+	+	+	+	+	+	+	-	+
^{7}Li(t,γ)^{10}Be	-	-	-	0	0	0	+	+	+
^{8}Li(t,n)^{10}Be	+	+	+	+	+	+	+	-	+
^{10}Be(t,n)^{12}B	-	0	+	-	0	+	-	0	+
^{10}Be(p,t)2^{4}He	-	-	-	-	-	-	-	-	-

7 Summary

This work has updated the BBN predictions in order to take into account the most recent developments concerning both the cosmological framework (i.e. the cosmological parameters determined from the recent CMB *Planck* experiment) and the microphysics. It demonstrates that these predictions are robust for the lightest elements. It shows also that the modification of these parameters in the range allowed cannot alleviate the lithium problem; concerning primordial CNO production we show that higher CNO yields can be expected: the four reaction rates ^{10}Be(α,n)^{13}C, ^{8}Li(t,n)^{10}Be, ^{10}Be(p,α)^{7}Li and ^{10}Be(p,t)2^{4}He, could be investigated to test this result.

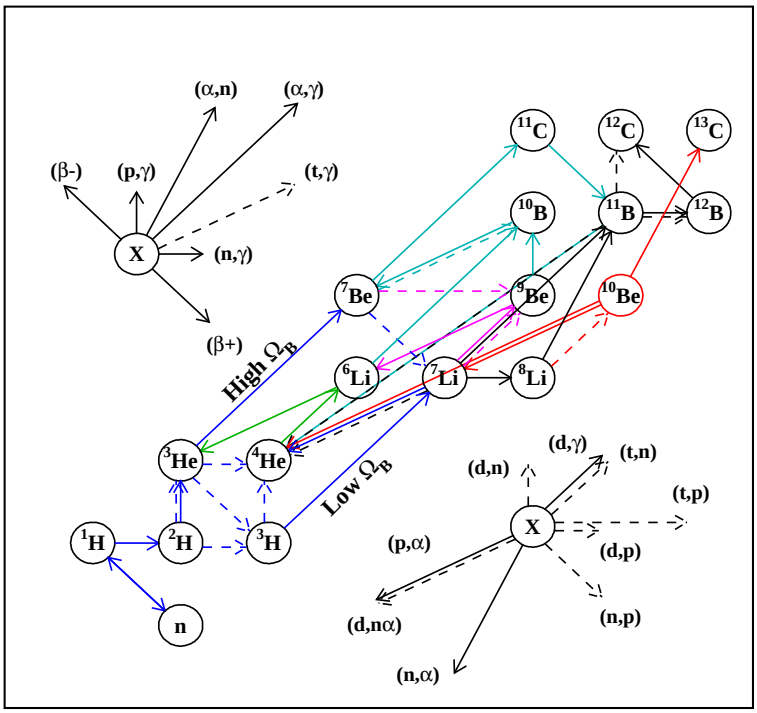

Figure 5. (Color online) BBN nuclear network with in red the new possible paths to CNO.

Acknowledgments

This work made in the ILP LABEX (under reference ANR-10-LABX-63) was supported by French state funds managed by the ANR within the Investissements d'Avenir programme under reference ANR-11-IDEX-0004-02 and by the ANR VACOUL, ANR-10-BLAN-0510.

A Appendix: Relation between η and $\Omega_{\rm b}h^2$

Here, for precise comparison with other works that quote η numerical values rather than $\Omega_{\rm b}h^2$ ones, we recall here the numerical relationship between the two.

What is important for BBN is the baryonic density $\Omega_{\rm b}{\cdot}\rho_{0,C}$ where $\rho_{0,C}$ is the present day critical density given by (numerical values of physical constants are taken from Beringer et al. [49]):

$$\rho_{0,C} = \frac{3H_0^2}{8\pi G} = 1.87847 \times 10^{-29}\ h^2\ {\rm g/cm^3}, \tag{A.1}$$

that allows for the calculation of

$$\rho_{\rm b}(t) = \left[1.87847 \times 10^{-29}\ {\rm g/cm^3}\right]\ \times\ \Omega_{\rm b}h^2 a^{-3}(t)\ , \tag{A.2}$$

to be used in the network calculations. The photon density (number/cm^3; $T_0 = 2.7255$ K; $\zeta(3) = 1.20206$) is:

$$n_\gamma(T) = \frac{2\zeta(3)}{\pi^2}\left(\frac{\mathrm{k_B}T}{\hbar c}\right)^3 = 410.73\left(\frac{T}{T_0}\right)^3 \ \mathrm{cm}^{-3} \tag{A.3}$$

The number of baryon per photon is thus given by:

$$\eta = \frac{\rho_{0,\mathrm{b}}}{n_\gamma(T_0)\bar{M}} \equiv \frac{3H_0^2}{8\pi G}\frac{\pi^2}{\zeta(3)}\left(\frac{\hbar c}{\mathrm{k_B}T_0}\right)^3\left(M_p(1-Y_p)+\frac{M_\alpha}{4}Y_p\right)^{-1}\Omega_\mathrm{b} \tag{A.4}$$

where $\bar{M}$ is the mean baryon mass

$$\bar{M} = M_p(1-Y_p)+\frac{M_\alpha}{4}Y_p = (1.6735 - 0.0119\ Y_p)\times 10^{-24}\ \ (g). \tag{A.5}$$

So that the relation between η and $\Omega_\mathrm{b}h^2$ are:

$$\eta = 2.7381\times 10^{-8}\ \Omega_\mathrm{b}h^2 \ \text{ or } \ \Omega_\mathrm{b}h^2 = 3.6521\times 10^7\ \eta \tag{A.6}$$

for Y_p=0.27 (solar, $\bar{M} = 1.6703\times 10^{-24}$ g) or

$$\eta = 2.7377\times 10^{-8}\ \Omega_\mathrm{b}h^2 \ \text{ or } \ \Omega_\mathrm{b}h^2 = 3.6528\times 10^7\ \eta \tag{A.7}$$

for Y_p=0.246 (BBN, $\bar{M} = 1.6706\times 10^{-24}$ g).

References

[1] S. Ando, R. H. Cyburt, S. W. Hong & C. H. Hyun, *Phys. Rev. C* **74** (2006) 025809

[2] C. M. Angulo, M. Arnould, M. Rayet, P. Descouvemont, D. Baye et al., *Nucl. Phys.*, A656 (1999) 3-183 and http://pntpm.ulb.ac.be/nacre.htm.

[3] M. Asplund, D.L. Lambert, P.E. Nissen, P.et al., *Astrophys. J.* **644** (2006) 229

[4] G. Audi, O. Bersillon, J. Blachot & A. H. Wapstra, *Nucl. Phys.* **A729** (2003) 3

[5] E. Aver, K. A. Olive& E. D. Skillman, *J. Cosmology Astropart. Phys.* **05**, (2010) 003

[6] E. Aver, K. A. Olive& E. D. Skillman, *J. Cosmology Astropart. Phys.* **04** (2012) 04

[7] E. Aver, K. A. Olive & E. D. Skillman, *J. Cosmology Astropart. Phys.* **11** (2013) 17

[8] T. Bania R. Rood & D. Balser, *Nature* **415** (2002) 54

[9] A. Boesgaard et al., *Astrophys. J.* **743** (2011) 140

[10] S. Cassisi & V. Castellani, *Astrophys. J. S.* **88** (1993) 509

[11] R. Cayrel, M. Steffen et al., *Astron. Astrophys.* **473** (2007) L37

[12] C. Charbonnel et al., *IAU Symposium 268, "Light Elements in the Universe", Cambridge University Press* **268** (2010)

[13] A. Coc & E. Vangioni, *J. of Physics Conference Series* **202** (2010) 012001

[14] A. Coc, S. Goriely, M. Saimpert, E. Vangioni & Y. Xu, *American Institute of Physics Conference Series* **1484** (2012) 354

[15] A. Coc, S. Goriely, Y. Xu, M. Saimpert & E. Vangioni, *Astrophys. J.* **744**, (2012)158

[16] A. Coc, J.-P. Uzan & E. Vangioni, *Phys. Rev. D* **87** (2013) 123530

[17] R. Cooke, M. Pettini, R. A. Jorgenson, M. T. Murphy & C. C. Steidel, *Astrophys. J.* **781** (2014) 31

[18] R. H. Cyburt & B. Davids, *Phys. Rev. C* **78** (2008) 064614

[19] R. H. Cyburt, J. Ellis, B. B. Fields et al., *J. Cosmology Astropart. Phys.* **05**, (2013) 14

[20] P. Descouvemont, A. Adahchour, C. Angulo, A. Coc & E. Vangioni-Flam, *Atomic Data and Nuclear Data Tables* **88**, (2004) 203

[21] D. Dicus, E. Kolb, A. Gleeson, E. Sudarshan, V. Teplitz & M. Turner, *Phys. Rev. D* **26** (1982) 2694

[22] D. Duncan et al., *Astrophys. J.* **488** (1997) 338

[23] S. Ekström, G. Meynet, C. Chiappini, R. Hirschi & A. Maeder, *Astron. Astrophys.* bf 489 (2008) 685

[24] B. D. Fields, *ARNPS* **6** (2011) 47

[25] A. Frebel & J. E. Norris, *published in 'Planets, stars and stellar systems', Springer, Edts T. Oswalt & G. Gilmore* **vol. 5** (2013) p. 55

[26] R. J. Garcia-Lopez et al., *Astrophys. J. Lett.* **500** (1998) 241

[27] S. Goriely, S. Hilaire, A. J. Koning, *Astron. Astrophys.***487** (2008) 767

[28] F. Hammache et al., *Phys. Rev. C* **82** (2010) 5803

[29] G. Hinshaw, D. Larson, E. Komatsu, E. et al., *Astrophys. J. S.* **208** (2013)19

[30] J. C. Howk, N. Lehner, B. D. Fields & G. J. Mathews, *Nature* **489** (2012) 121

[31] C. Iliadis, R. Longland, A. E. Champagne, J. R. Newton, C. Ugalde, A. Coc &R. Fitzgerald, *Nucl. Phys.*, **A841** (2010) 31

[32] F. Iocco, P. Bonifacio & E. Vangioni, *Proceedings of the workshop* Lithium in the cosmos, *Mem.S.A.It. Suppl.* **22** (2012) 3

[33] F. Iocco, G. Mangano, G. Miele, O. Pisanti & P. D. Serpico, *Phys. Rev. D* **75** (2007) 30141

[34] Y. I. Izotov & T. X. Thuan, *Astrophys. J. Lett.* **710** (2010) L67

[35] Y. I. Izotov, G. Guseva, K. J. Fricke & C. Henkel, *Astron. Astrophys.* **561** (2013) 33

[36] E. Komatsu et al., *Astrophys. J. S.* **192**, (2011) 18

[37] K. Lind, J. Melendez, M. Asplund et al., *Astron. Astrophys.* **554** (2013) 96

[38] R. Longland, C. Iliadis, A. E. Champagne et al., *Nucl. Phys.* A **841** (2010) 1

[39] R. E. Lopez & M. S. Turner, *Phys. Rev. D* **59** (1999) 103502

[40] G. Mangano et al, *Nucl. Phys.* B **729** (2005) 221

[41] K. A. Olive, P. Petitjean, E. Vangioni & and J. Silk, *Mon. Not. R. Astron. Soc.* **426** (2012) 1427

[42] A. Parikh, J. José, F. Moreno, & C. Iliadis, *Astrophys. J. S.* **178** (2008) 110

[43] P. Peter & J.-P. Uzan, *Primordial Cosmology* (Oxford University Press) (2009)

[44] M. Pettini, B. J. Zych, M. Murphy, A. Lewis & C. C. Steidel *Mon. Not. R. Astron. Soc.* **391** (2008) 1499

[45] M. Pettini & M. Cooke, *Mon. Not. R. Astron. Soc.* **425** (2012) 2477

[46] R.G. Pizzone, R. Sparta, C.A. Bertulani, C. Spitaleri, M. La Cognata, J. Lalmansingh, L. Lamia, A. Mukhamedzhanov & A. Tumino `(arXiv:1403.4909[nucl-ex])`, *to appear in Astrophys. J.*

[47] *Planck* Collaboration XVI, P. A. R. Ade, N. Aghanim et al., arXiv:1303.5076 (2013)

[48] The Review of Particle Physics, C. Amsler et al., (Particle Data Group) *Phys. Lett.* B **667** (2008) 1

[49] The Review of Particle Physics, J. Beringer et al., (Particle Data Group) *Phys. Rev. D* **86** (2012) 010001

[50] E. Rollinde, E.Vangioni & K. A. Olive, *Astrophys. J.* **627** (2005) 666

[51] S. G. Ryan, T. C. Beers, K. A. Olive, B. D. Fields & J. E. Norris, *Astrophys. J.* **530** (2000) L57

[52] A. L. Sallaska, C. Iliadis, A. E. Champagne et al., *arXiv:1304.7811* (2013)

[53] L. Sbordone et al., *Astron. Astrophys.* **522** (2010) 26

[54] A. Serebrov, V. Varlamov & A. Kharitonov et al., *Phys. Lett.* B **605** (2005) 72

[55] D. N. Spergel et al., *Astrophys. J. S.* **170** (2007) 377

[56] D.N. Spergel, R. Flauger & R. Hložek, (`arXiv:1312.3313v1[astro-ph.CO]`)

[57] F. Spite & M. Spite, *Astron. Astrophys.* **115** (1982) 357

[58] F. Spite & M. Spite, Proceedings IAU Symposium No. 268, *Light Elements in the Universe 9-13 November, Geneva, Switzerland, Eds. C. Charbonnel, M. Tosi, F. Primas & C. Chiappini, Cambridge University Press* (2010) p. 201

[59] M. Steffen, R. Cayrel, E. Caffau et al., Mem. Soc. Astron. It. Suppl. **22** (2012) 152

[60] E. Vangioni-Flam, M. Cassé, B. D. Fields & K. A. Olive, *Astrophys. J.* **468** (1996) 199

[61] E. Vangioni-Flam, R. Ramaty, K. A. Olive & M. Cassé, *Astron. Astrophys.* **337** (1998) 714

[62] E. Vangioni-Flam, M. Cassé & J. Audouze, *Physics Reports* **333** (2000) 365

[63] E. Vangioni-Flam & M. Cassé, *New Astr. Rev.* **45** (2001) 583

[64] E. Vangioni-Flam et al., *Astrophys. J.* **585** (2003) 611

[65] B. Wang, C. A. Bertulani and A. B. Balantekin, *Phys. Rev. C* **83** (2011) 018801

[66] F. Wietfeldt & G. Greene, *Rev. Mod. Phys.* **83** (2011) 1173

[67] Y. Xu, K. Takahashi, S. Goriely, M. Arnould, M. Ohta & H. Utsunomiya, *Nucl. Phys.* A **918** (2013) 61

[68] A. T. Yue, M. S. Dewey & D.M. Gilliam, *Phys. Rev. Lett.* **111** (2013) 222501